PHYSICAL REVIEW A VOLUME 24, NUMBER 6 DECEMBER 1981

Inner-shell analytic relativistic radiative transition rates in screened potentials

Oscar V. Gabriel, Siddheswar Chaudhuri, and R. H. Pratt
Department of Physics and Astronomy, University of Pittsburgh, Pittsburgh, Pennsylvania 15260
(Received 27 July 1981)

Analytic expressions are obtained for relativistic radiative-decay rates of transitions between the L and K shells of intermediate- and high-Z elements. These single-electron transition rates in a central potential can be expressed as a power series in the atomic scale parameter λ which characterizes a small-distance expansion of the relativistic screened atomic potential. Retardation effects and all multipole contributions of the radiation field are included. With this approach it is possible to trace explicitly, both for the point Coulomb potential and for screening modifications, the role of relativistic, retardation, and higher multipole contributions in modifying the corresponding nonrelativistic dipole transition rates.

I. INTRODUCTION

An inner-shell (here K-shell) atomic vacancy may be filled by an electron from an outer shell (here L shell) in a transition accompanied either by photon emission (radiative decay) or by the Auger effect (ejection of another atomic electron). Decay by photon emission, which is considered in this paper, results in the characteristic x-ray spectra. The emission spectrum from an atom or ion can be analyzed to provide a variety of information about the emitting system and its environment. Such analysis depends on precision of predictions for the basic rates, so that relativistic corrections to the usual nonrelativistic dipole calculations are often needed. Our purpose here is to develop realistic analytic relativistic expressions for these rates for inner-shell transitions, permitting both a simple characterization of photon emission and an understanding of the origins of its features.

There have been numerous calculations of relativistic radiative rates, including the works of Massey and Burhop,[1,2] Laskar,[3,4] Payne and Levinger,[5] Asaad,[6] Taylor and Payne,[7] Babushkin,[8–10] Grant,[11] Garstang,[12] Rosner and Bhalla,[13] Anholt and Rasmussen,[14] Lu, Malik, and Carlson,[15] and Scofield.[16–18] The more recent approaches are based on computer-calculated Hartree-Fock self-consistent many-electron wave functions. In this paper, we follow closely the formulation of Scofield,[16,17] who has reported the results from numerical calculations of x-ray emission rates due to an electron filling a single vacancy in either the K or the L shell. Scofield's work is based on single-particle states in a central potential given by the relativistic Dirac-Hartree-Slater theory and yields results which are in good agreement with experiment.

The emphasis in many atomic calculations is on transitions of outer electrons, for which the major problem is the complexity of the treatment of electron-electron correlations. In dealing with inner-shell transitions, the importance of electron-electron interactions is diminished in comparison to electron-nucleus interaction; it is reasonable to expect that simpler treatments will yield valid results and that perturbation techniques for effects beyond the electron-nucleus interaction will be useful.[17] However, for inner-shell transitions in higher-Z elements, relativistic effects and retardation corrections (due to the finite x-ray wavelength) lead to important modifications. Further, higher radiation multipoles, in addition to the dominant electric-dipole term, play an increasing role as we go to higher nuclear charge Z and to higher inner-shell transition energies.

In this paper we report explicit analytic expressions for the rates of transitions from the L to the K shell, assumed to have initially a single vacancy. We give fully relativistic closed-form expressions for the first terms of a perturbation expansion in the atomic scale parameter λ for $K\alpha_1$, $K\alpha_2$, and KL_1 emission as functions of Z. Our calculations are based on a description for single-electron transitions between states of definite total angular momentum and energy. With these analytic results, broad surveys are easily achieved, which otherwise would require extensive numerical calculations. Further, the dependence of the transition

rates on relevant parameters such as Z and Z_i (degree of ionization) can be studied more readily. The approach also allows the separation of the consequences of different effects such as relativity, screening, retardation, and presence of higher multipoles, and hence it can provide some physical insight into the underlying mechanisms of the process.

Our work utilizes the analytic wave functions provided by the relativistic version of an analytic perturbation theory (APT) for screened-Coulomb potentials, as discussed by McEnnan *et al.*,[19] based on a series expansion of a smoothed screened atomic potential in the interior of the atom. This theory is known to give good approximate wave functions and energy eigenvalues particularly for inner-shell electrons. The present work represents one of the first applications of the relativistic APT in the calculations of atomic processes.

In Sec. II we discuss briefly the formulation of the relativistic radiative transition matrix element and the transition probability. In Sec. III (and in the Appendix) we review the needed results of the relativistic APT, presenting explicitly (up to the third order in the expansion parameter λ) the wave functions, normalization constants, and energy eigenvalues. We also verify that these expressions reduce to the proper nonrelativistic results in the limit of small $a \equiv \alpha Z$. Section IV gives the main results of this paper, namely, the relativistic analytic transition rates. As one check of these results we investigate the various limiting cases. We also compare the predictions of our expressions with the numerical results of Scofield; the good agreement achieved is a further demonstration of the validity of the analytic forms. In Sec. V we then utilize the analytic expressions to study the interplay of relativistic, screening, retardation, and multipole effects in modifying the simple and familiar nonrelativistic dipole hydrogenic transition rates.

II. FORMULATION OF THE TRANSITION RATES

We follow standard procedure and use the Feynman-Dyson formulation of quantum electrodynamics. The atomic field, included in the unperturbed Hamiltonian, is assumed to be a central potential. The transition probability W_{ab} is obtained from the matrix element of the S operator between initial and final states of the radiating system. Using natural units in which $h = m_e = c = 1$,

$$W_{ab} = \frac{\alpha K}{2\pi} \sum_{\text{pol}} \int d\Omega_K \, | \langle a | \vec{\alpha} \cdot \hat{\epsilon} e^{i \vec{K} \cdot \vec{r}} | b \rangle |^2 , \tag{1}$$

where the initial and final atomic bound states are labeled a and b, respectively; $\vec{K}$ is the photon momentum and in the units used, $K = E_a - E_b$ where E is the energy eigenvalue. [See Rose and Brink[20] for a derivation of Eq. (1).] We shall assume that the initial subshell is completely filled and the final subshell has only one vacancy. In our general calculations we shall leave K as a free parameter, so that for a given choice of gauge we could explore the role of retardation separately from relativity.

Making a multipole expansion of the radiation field operator in the matrix element of Eq. (1) and performing the angular integrals and the average over the quantum numbers of the initial state (see Scofield[16]),

$$W_{ab} = 2\alpha K^2 \sum_{L=1}^{\infty} [f_L(m) + f_L(e)] , \tag{2}$$

where $f_L(m)$ is the oscillator strength due to the 2^L-pole-type magnetic interaction and $f_L(e)$ is the corresponding term due to the electric interaction. Selection rules allow only a small discrete set of terms from the infinite series in Eq. (2) for the case of a bound-bound transition. The oscillator strengths are given as

$$f_L(m) = n_a B(-\kappa_a, \kappa_b, L) R_L^2(m)/K , \tag{3a}$$

$$f_L(e) = n_a B(\kappa_a, \kappa_b, L) R_L^2(e)/K , \tag{3b}$$

where

$$B(\kappa_a, \kappa_b, L) = \frac{(2l_a+1)(2l_b+1)}{L(L+1)} \times C^2(l_a, l_b, L; 0, 0) \times D^2(j_a, l_a\, j_b l_b; \tfrac{1}{2} L) ,$$

$$j = |\kappa| - \tfrac{1}{2}; = \begin{cases} \kappa, & \kappa > 0 \\ -\kappa - 1, & \kappa < 0 \end{cases} .$$

κ is the Dirac quantum number, C and D are angular factors (see Scofield[16] for the definitions), and n_a is the number of electrons in the initial subshell ($n_a = 2j_a + 1$ for a filled subshell). For a transition between single-particle states in a central potential, the radial matrix elements R_L can be written in terms of the radial wave functions f (large com-

ponent), g (small component), and the spherical Bessel function $j_L(Kr)$:

$$R_L(m)=(\kappa_a+\kappa_b)\int_0^\infty j_L(Kr)P_+(r)dr\ , \tag{4a}$$

$$R_L(e)=\int_0^\infty j_{L-1}(Kr)\times[(\kappa_b-\kappa_a)P_+(r)+LP_-(r)]dr+\int_0^\infty j_L(Kr)Q(r)dr\ , \tag{4b}$$

where

$$P_\pm(r)=g_b(r)f_a(r)\pm f_b(r)g_a(r)\ ,$$

$$Q(r)=f_b(r)f_a(r)+g_b(r)g_a(r)\ .$$

These are the basic objects to be computed. There are other equivalent formulas as given by various authors[10–13] who use other gauges. (See the work of Grant[11] for a general discussion of the dependence of the matrix elements on the gauge in which the electromagnetic potentials are written.) The radial wave functions satisfy the coupled differential equation (Dirac)

$$\left[\frac{d}{dr}+\frac{\kappa}{r}\right]f=(E+1-V)g,$$

$$\left[-\frac{d}{dr}+\frac{\kappa}{r}\right]g=(E-1-V)f\ , \tag{5}$$

and are normalized so that

$$\int_0^\infty (f^2+g^2)dr=1\ .$$

Note that f and g so defined are multiplied by r in comparison to the forms often used.

III. WAVE FUNCTIONS

The relativistic version of the analytic perturbation theory (APT) expresses the functions f and g in terms of decaying exponentials and polynomials in r. These provide series solutions in λ for the radial Dirac equations, Eqs. (5), in a screened central potential expressed in the form

$$rV(r)=-a\sum_{n=0} V_n(\lambda r)^n,\quad V_0\equiv 1 \tag{6}$$

where $a=\alpha Z$, α is the fine-structure constant and $\lambda\equiv\lambda(Z)$ is a small parameter (λ^{-1} scales the size of the atom). The coefficients V_n characterize the atomic screening and can be chosen such that the sum converges rapidly and gives a good approximation to a smoothed realistic potential in the interior region of an atom. Energy eigenvalues and normalization constants, as well as the radial wave functions, can be expressed as a series in λ with simple analytic coefficients; these expressions as well as their nonrelativistic reductions are given in the Appendix. We will write our main results in terms of the reduced functions F_1 and F_2 rather than f and g, where

$$f=Nr^\gamma e^{-p_c r}\left[\frac{1+E_c}{2}\right]^{1/2}(F_1+F_2)\ ,$$

$$g=Nr^\gamma e^{-p_c r}\left[\frac{1-E_c}{2}\right]^{1/2}(F_1-F_2)\ . \tag{7}$$

In Eq. (7), N is the screened normalization constant, $\gamma=(\kappa^2-a^2)^{1/2}$ is the Dirac constant, E_c is the Coulomb eigenenergy, and $p_c=(E_c^2-1)^{1/2}$.

Figure 1 shows comparisons between analytic wave functions for $2p_{1/2,3/2}$ bound states and numerical calculations and relativistic and nonrela-

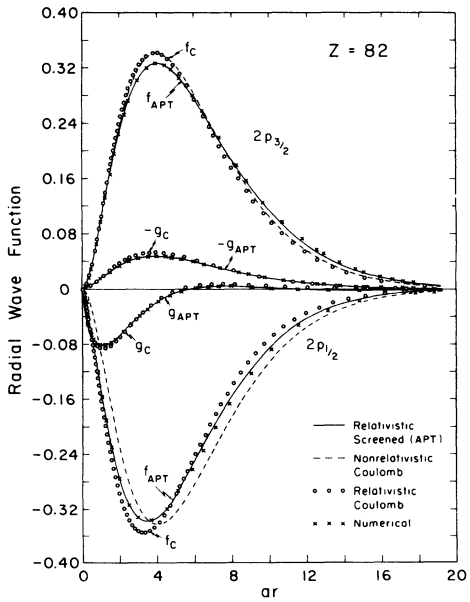

FIG. 1. Radial part of relativistic $2p_{3/2}$ and $2p_{1/2}$ wave functions versus radial distance scaled by $a\equiv\alpha Z$. Solid lines represent large and small components, obtained from our analytic expressions using the HFS (Liberman) potential with the Kohn-Sham exchange term and the Latter tail correction, broken lines represent nonrelativistic Coulomb radial wave functions. Relativistic Coulomb values (○) and numerical screened relativistic values (×) are also shown.

tivistic wave functions. Other cases were shown previously.[19] We see that the APT provides a good approximation for these relativistic screened wave functions.

IV. ANALYTIC TRANSITION RATES

A. Transition $2p_{3/2}\rightarrow 1s_{1/2}$ ($K\alpha_1$)

To illustrate our method we begin with the derivation of the analytic transition rate for the $K\alpha_1$ line of the characteristic x-ray spectrum. By using the properties of the angular factor $B(\kappa_a,\kappa_b,L)$, we find that the nonvanishing value $B(-2,-1,1)=\frac{1}{4}$ occurs in $f_1(e)$ and $B(2,-1,2)=\frac{1}{12}$ occurs in $f_2(m)$. The relevant radial matrix elements are

$$R_1(e)=2J_0+J_{1f}+J_{1g},\quad R_2(m)=-3J_2\ , \tag{8}$$

where

$$J_0=\int j_0 g_b f_a dr,\quad J_{1f}=\int j_1 f_b f_a dr\ ,$$
$$J_{1g}=\int j_1 g_b g_a dr,\quad J_2=\int j_2 P_+ dr\ . \tag{9}$$

These integrals can be written in terms of the reduced functions F_1 and F_2 defined in Eq. (7),

$$J_0=C\mu_{(-)}^{(b)}\mu_{(+)}^{(a)}[I_{12}^{(0)}-I_{21}^{(0)}-I_{22}^{(0)}]\ ,$$
$$J_{1f}=C\mu_{(+)}^{(b)}\mu_{(+)}^{(a)}[I_{12}^{(1)}+I_{21}^{(1)}+I_{22}^{(1)}]\ ,$$
$$J_{1g}=C\mu_{(-)}^{(b)}\mu_{(-)}^{(a)}[-I_{12}^{(1)}-I_{21}^{(1)}+I_{22}^{(1)}]\ , \tag{10}$$
$$J_2=C[\lambda_{(-)}(I_{12}^{(2)}-I_{21}^{(2)})-\lambda_{(+)}I_{22}^{(2)}]\ ,$$

where

$$I_{ij}^{(L)}=\int_0^\infty j_L(Kr)e^{-pr}r^{\gamma_a+\gamma_b}F_i^{(b)}F_j^{(a)}dr,\quad L=0,1,2, \tag{11}$$

and

$$p=p_{ca}+p_{cb},\quad C=\tfrac{1}{2}N_bN_a\ ,$$
$$\mu_{(\pm)}=(1\pm E_c)^{1/2},\quad \lambda_{(\pm)}=\mu_{(-)}^{(b)}\mu_{(+)}^{(a)}\pm\mu_{(+)}^{(b)}\mu_{(-)}^{(a)}\ .$$

We have neglected $I_{11}^{(L)}$ in Eq. (1) since it is of order λ^4 and we have retained terms only through $O(\lambda^3)$. In general, F_i is a series in λ having coefficients which are simple polynomials in r. Consequently, $I_{ij}^{(L)}$ can be evaluated in closed form. We utilize the formulas

$$\int_0^\infty j_0(Kr)e^{-pr}r^\beta dr=\frac{\Gamma(\beta)\sin\beta\phi}{C^{\beta+1}\sin\phi}\ , \tag{12a}$$

$$\int_0^\infty j_1(Kr)e^{-pr}r^\beta dr=\frac{\Gamma(\beta+2)}{2\beta C^{\beta+1}\sin^2\phi}\left[\frac{\sin(\beta-1)\phi}{\beta-1}-\frac{\sin(\beta+1)\phi}{\beta+1}\right]\ , \tag{12b}$$

$$\int_0^\infty j_2(Kr)e^{-pr}r^\beta dr=\frac{\Gamma(\beta+3)}{4\beta C^{\beta+1}\sin^3\phi}\left[\frac{\sin(\beta-2)\phi}{(\beta-1)(\beta-2)}-\frac{2\sin\beta\phi}{(\beta-1)(\beta+1)}+\frac{\sin(\beta+2)\phi}{(\beta+1)(\beta+2)}\right]\ , \tag{12c}$$

where $C=(p^2+K^2)^{1/2}$ and $\tan\phi=K/p$. The expressions for $I_{ij}^{(L)}$ are given in the Appendix. The transition rate is

$$W_{K\alpha_1}=2\alpha k[R_1^2(e)+\tfrac{1}{3}R_2^2(m)]\ . \tag{13}$$

B. Transition $2p_{1/2}\rightarrow 1s_{1/2}$ ($K\alpha_2$)

For the $K\alpha_2$ line, all magnetic multipoles vanish since $\kappa_a+\kappa_b=0$. The only nonvanishing angular coefficient is $B(1,-1,1)=\frac{1}{4}$ and the term that survives in Eq. (2) is the electric-dipole oscillator strength $f_1(e)$. The only radial matrix element that has to be evaluated is

$$R_1(e)=J_{if}+J_{ig}-J_0-3J_0'\ , \tag{14}$$

where J_0, J_{1f}, and J_{1g} are defined in Eq. (8), while

$$J_0'=\int_0^\infty j_0 f_b g_a dr\ . \tag{15}$$

In terms of integrals of the reduced radial wave functions

$$J_{1f}=C\mu_{(+)}^{(b)}\mu_{(+)}^{(a)}[I_{11}^{(1)}+I_{12}^{(1)}+I_{21}^{(1)}+I_{22}^{(1)}]\ ,$$
$$J_{1g}=C\mu_{(-)}^{(b)}\mu_{(-)}^{(a)}[I_{11}^{(1)}-I_{12}^{(1)}-I_{21}^{(1)}+I_{22}^{(1)}]\ ,$$
$$J_0=C\mu_{(-)}^{(b)}\mu_{(+)}^{(a)}[I_{11}^{(0)}+I_{12}^{(0)}-I_{21}^{(0)}-I_{22}^{(0)}]\ , \tag{16}$$
$$J_0'=C\mu_{(+)}^{(b)}\mu_{(-)}^{(a)}[I_{11}^{(0)}-I_{12}^{(0)}+I_{21}^{(0)}-I_{22}^{(0)}]\ .$$

The $I_{ij}^{(L)}$ are given in the Appendix. The transition rate is

$$W_{K\alpha_2}=\alpha K R_1^2(e) . \tag{17}$$

C. Transition $2s_{1/2}\rightarrow 1s_{1/2}$ (KL_1)

The process we are considering here is the emission of a single $M1$ photon (rather than two $E1$ photons) in an optically forbidden transition. The relevant radial matrix element is

$$R_1(m)=(\kappa_a+\kappa_b)\int_0^\infty j_1 P_+ dr$$
$$=-2C[\lambda_{(+)}(I_{22}^{(1)}-I_{11}^{(1)})+\lambda_{(-)}(I_{21}^{(1)}-I_{12}^{(1)})] \tag{18}$$

and the transition rate

$$W_{KL_1}=\alpha K R_1^2(m) . \tag{19}$$

D. Nonrelativistic (small αZ) limits for $K\alpha$ transitions

As one check of our analytic results, we extract their nonrelativistic limits. First we consider the optically allowed transitions $2p_{3/2}$, $2p_{1/2}\rightarrow 1s_{1/2}$. For small K, we find that the $M2$ contribution $R_2(m)$ becomes small compared to the dominant $R_1(e)$ since

$$j_L(Kr)\sim (Kr)^L/(2L+1)!!$$

and, in fact,

$$[R_1(e)]_{K\alpha_1,K\alpha_2}\rightarrow -\tfrac{2}{3}K\int_0^\infty (f_b f_a+g_b g_a) r\, dr , \tag{20}$$

where we have used the identity (see Grant[11] and Garstang[12])

$$\frac{d}{dr}(g_b f_a-f_b g_a)+\frac{\kappa_a-\kappa_b}{r}(g_b f_a+f_b g_a)$$
$$=K(f_b f_a+g_b g_a) .$$

Then letting $a=\alpha Z\rightarrow 0$ under the integral (which is consistent with having kept only the leading order in K) we may neglect $g_b g_a$ and replace the large component f by rR, where R is the corresponding solution of the radial Schrödinger equation. In this limit $R_1(e)$ is proportional to the nonrelativistic matrix element M,

$$[R_1(e)]_{\kappa\alpha_1,\kappa\alpha_2}\rightarrow -\tfrac{2}{3}KM,\quad M=\int_0^\infty R_b^* r R_a r^2 dr , \tag{21}$$

giving results in agreement with Kim *et al.* and other authors.[11,12,17]

Also in this limit the optical oscillator strengths (OOS) obtained from Eq. (3b) obey the relation[5]

$$f_{K\alpha_1}+f_{K\alpha_2}=f_{\rm NR} , \tag{22}$$

where $f_{\rm NR}=\frac{2}{3}KM^2$ is the familiar nonrelativistic OOS. The transition rates of Eqs. (12) and (16) reduce to

$$W_{K\alpha_1}=2W_{K\alpha_2}=\tfrac{8}{9}\alpha K^3 M^2 , \tag{23}$$

where $K=K_C S_K$, $M=M_C S_M$. For $K\alpha$ transitions, the nonrelativistic Coulomb expressions are $K_C=3a^2/8$ and $M_C=2^{15/2}/3^{9/2}a$, while the screening correction factors are

$$S_K=1-28\Lambda_2/3-72\Lambda_3 ,$$
$$S_M=1-23\Lambda_2/2-3059\Lambda_3/18 ,$$

with $\Lambda_n\equiv V_n\lambda^n/a^n$. These nonrelativistic results allow quick estimates of the magnitude of the $2p\rightarrow 1s$ transition rates.

It is interesting to examine the first corrections to the nonrelativistic decay rates. If the next order contribution in $a=\alpha Z$ is kept, we get in the Coulomb case

$$W_{K\alpha_1}=(2^9\alpha a^4/3^8)[1-a^2(\tfrac{7}{24}+\ln 32-\ln 27)/2]$$
$$\approx 291.0(1-0.231a^2)a^4\,{\rm eV}/\hbar , \tag{24a}$$

$$W_{K\alpha_2}=(2^8\alpha a^4/3^8)[1+a^2(\tfrac{1}{64}+\ln 9-\ln 8)]$$
$$\approx 145.5(1+0.133a^2)a^4\,{\rm eV}/\hbar , \tag{24b}$$

which gives the order a^2 corrections due to relativity and retardation (higher multipole contributions do not enter in this order). The coefficients are small, so that nonrelativistic dipole approximation remains fairly good even for high-Z elements. Note that the shifts are in opposite directions so that there is further cancellation when we consider the total transition rate.

$$W(2p\rightarrow 1s)$$
$$=(2^8\alpha a^4/3^7)[1-a^2(\tfrac{55}{192}+\ln 256-\ln 243)/3]$$
$$\approx 436.5(1-0.113a^2)a^4\ {\rm eV}/\hbar . \tag{24c}$$

This provides another illustration of the extended validity of the nonrelativistic dipole approximation.

E. Nonrelativistic (small αZ) limit for KL_1 transition

One must be careful in taking the "nonrelativistic limit" of the KL_1 analytic transition rate. As mentioned previously, this transition is optically forbidden (being of the $M1$ type). Breit and Teller[21] have pointed out that this rate vanishes in the nonrelativistic limit. However, it is still possible to extract the leading term in an expansion in αZ. The contribution of the leading term in the small-K expansion for the spherical Bessel function $j_1(Kr)$ vanishes identically in the nonrelativistic limit because of the orthogonality of the Coulomb-Schrödinger radial s-state wave functions. Consequently, in order to correctly obtain the leading nonvanishing contributions in the small-a limit, higher-order terms in *both* $j_1(Kr)$ and the Dirac wave functions must be considered. However, estimating the $2s\rightarrow 1s$ transition rate in hydrogen, Garstang[12] made the replacement $j_1(Kr)\rightarrow Kr/3$ while keeping relativistic corrections in the wave functions and obtained the result

$$W_{KL_1}=\alpha a^{10}/432=5.62\times 10^{-6}Z^{10}\ \text{sec}^{-1}. \tag{25a}$$

This ignores the next term in $j_1(Kr)$ which gives a contribution of the same order in a. By contrast Grant, in his review article,[22] gave another estimate (which he cautioned was not based on an adequate calculation)

$$W_{KL_1}=\alpha a^{10}/3888=0.613\times 10^{-6}Z^{10}\ \text{sec}^{-1}, \tag{25b}$$

obtained by retaining the two leading terms of $j_1(Kr)$ but only the leading term of the wave functions. The correct lowest-order result, in fact, lies between these two values.

In taking the small-a limit for this transition, we simplify the discussion by keeping only the point Coulomb term (i.e., we set $\Lambda_2=\Lambda_3=0$). Then from Eq. (17),

$$R_1(m)=C(\lambda_{(+)}A+\lambda_{(-)}B), \tag{26}$$

where

$$C=-2N_bN_a[\gamma(\eta'-1)]^{1/2},\quad \lambda_{(\pm)}=a(\eta'+2\pm\eta')/\eta'(\eta'+2)^{1/2},$$

$$A=[(2(\gamma+1)G(2\gamma)-2aG(2\gamma+1)/\eta']/(\eta'+1),\quad B=-G(2\gamma),$$

$$G(x)=\int_0^\infty j_1(Kr)e^{-pr}r^x dr=\frac{K}{3}\frac{\Gamma(x+2)}{p^{x+2}}F\left[\frac{x+2}{2},\frac{x+3}{2};\frac{5}{2};\frac{-K^2}{p^2}\right],$$

and F is the hypergeometric function. Equation (26) is equivalent to the closed-form result given by Johnson.[23] Now for small K,

$$G(x)\rightarrow\frac{K}{3}\frac{\Gamma(x+2)}{p^{x+2}}\left[1-\tfrac{1}{10}(x+2)(x+3)\frac{K^2}{p^2}\right], \tag{27}$$

so that with the replacements $K\rightarrow\frac{3}{8}a^2(1+\frac{11}{48}a^2)$, $p\rightarrow\frac{3}{2}a(1+\frac{1}{24}a^2)$, $\gamma\rightarrow 1-\frac{1}{2}a^2$, and $\eta'\rightarrow 2-\frac{1}{4}a^2$ we have

$$R_1(m)\rightarrow -2^{1/2}a^4/27,$$

$$W_{KL_1}\rightarrow\alpha a^{10}/972\approx 2.4958\times 10^{-6}Z^{10}\ \text{sec}^{-1}, \tag{28}$$

in agreement with the result obtained by Johnson[23] and also by other authors.[24–26] Note that Garstangs's limit Eq. (25a) corresponds to retaining only the leading term of $G(x)$ in Eq. (27). However, one can verify that in combining the leading terms to get $R_1(m)$, an expression which is two orders higher in $a=\alpha Z$ will result and therefore both terms in Eq. (27) must be included.

F. Comparison with numerical calculations

In order to further establish the validity of the analytic approach and the correctness of its calculation, we compare our results with Scofield's numerical calculations.[16–18] The graphs shown in Fig. 2 show the relative transition rates (a relative transition rate is obtained by taking the ratio of the rate to the corresponding nonrelativistic Coulomb rate $W_{\text{NRC}}=2^9\alpha a^4/3^8$, $2^8\alpha a^4/3^8$, $\alpha a^{10}/972$ for $K\alpha_1$, $K\alpha_2$, KL_1, respectively) as functions of the nuclear charge Z. Data for representative elements are also shown in Table I. All the Coulomb results of course approach the W_{NRC} values for small a; we see that, in agreement with Eq. (28), $W_{K\alpha_1}$ approaches from below and $W_{K\alpha_2}$ approaches from above. The screened $K\alpha$ rates also merge to a

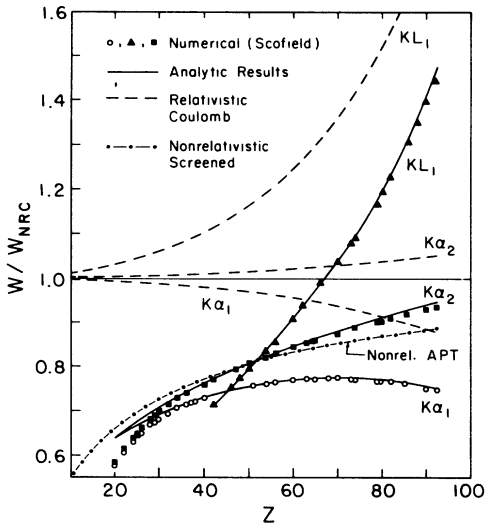

FIG. 2. Transition rate, W normalized by the corresponding small-a limit Coulomb values, W_{NRC} as a function of the nuclear charge Z. The solid lines represent our relativistic analytic screened results while the broken lines represent relativistic Coulomb results. The dash-dotted line corresponds to the nonrelativistic screened (APT) results. Circles, squares, and triangles are the numerical results of Scofield for $K\alpha_1$, $K\alpha_2$, and KL_1 transitions, respectively, to be compared with the solid lines.

common nonrelativistic case for small a. As one would expect, screening causes larger effect for small $Z\alpha$ than for large $Z\alpha$, where the shells are more interior and Coulomb-like.

The analytic perturbation-theory results agree very well with those of Scofield, within 1% for $K\alpha_1$, $K\alpha_2$ and within 3% for KL_1 in the medium- and high-Z elements. (Improved predictions are obtained for the analytic KL_1 rates if numerical rather than analytic normalizations are used, as shown in Fig. 2. This appears to occur because the transition is characterized by distances for which screening enters primarily through the $2s$ normalization, which is relatively slowly converging within APT). Significant deviations from the numerical values occur only for the light elements (for which APT wave functions are not accurate). We thus verify the adequacy of the analytic perturbation theory for the prediction of these inner-shell transition rates. We may therefore use the analytic forms to explore the role of various mechanisms (screening, relativity, retardation, higher multipoles, etc.) in determining the rates.

V. DISCUSSION OF RESULTS

Knowing the accuracy of the APT transition rate formalism, we may then employ it (as well as numerical calculations) to identify those features of the calculation that are important in determining the observed rates. We may study the effects of such features as (i) screening, (ii) relativity, (iii) retardation, and (iv) higher multipoles in the radiation field. As we will discuss subsequently, (ii) and (iii) are linked through the choice of the gauge.

TABLE I. Sample results for transition rates (in eV/$\hbar$) of atoms filling a vacancy in the K shell.

		Relativistic results				Nonrelativistic results			
		Analytic perturbation-theory		Numerical		Analytic perturbation theory			
Z	Transition	with V_{rel}	with V_{nonrel}	(Scofield)	Coulomb	with V_{rel}	with V_{nonrel}	Numerical	Coulomb
92	$K\alpha_1$	44.66	46.17	44.19	52.00	50.69	52.30	51.08	59.11
	$K\alpha_2$	27.95	28.66	27.61	31.11	25.35	26.17	25.54	29.56
	KL_1	0.105	0.109	0.103	0.128				0.0714
82	$K\alpha_1$	28.71	29.62	28.49	33.88	31.63	32.57	31.72	37.31
	$K\alpha_2$	17.10	17.55	16.95	19.45	15.81	16.29	15.86	18.65
	KL_1	0.0280	0.0292	0.0277	0.0352				0.0226
50	$K\alpha_1$	3.897	4.001	3.890	4.994	4.072	4.168	3.994	5.157
	$K\alpha_2$	2.079	2.133	2.080	2.620	2.036	2.084	1.997	2.579
	KL_1	0.128(−3)	0.132(−3)	0.127(−3)	0.186(−3)				0.160(−3)
26	$K\alpha_1$	0.2525	0.2566	0.244	0.3739	0.2639	0.2672	0.2371	0.3771
	$K\alpha_2$	0.1284	0.1306	0.1248	0.1893	0.1318	0.1336	0.1190	0.1880

We may begin to explore the consequences of (i)—(iv) by obtaining from our analytic expressions the transition rates corresponding to relativistic screened and Coulomb and to nonrelativistic screened and Coulomb calculations. [The nonretarded dipole approximation, with $\exp(i\vec{K}\cdot\vec{r})$ replaced by $(1+i\vec{K}\cdot\vec{r})$ and only the lowest nonvanishing order in K kept, is assumed in all nonrelativistic results.] Table I gives the results of these calculations. Note that all the features (i)—(iv) are included in our complete relativistic calculation whereas all of them are omitted in the simplest approach, the nonrelativistic nonretarded Coulomb dipole approximation. Screening tends to decrease the rates; relativity and retardation, as already noted, increase $K\alpha_2$ and decrease $K\alpha_1$. The higher multipole effect (iv) is of minor importance. In high-Z elements the reductions due to screening and effects due to retardation and relativity are of comparable magnitude (canceling for $K\alpha_2$ and adding for $K\alpha_1$), while in lighter elements the screening effects are more important. These can be seen in Fig. 2.

As noted above, screening causes a reduction of the Coulomb rates, similar in character in both the relativistic and nonrelativistic cases (refer to Table II). Evidently, the relativistic corrections to screening effects are a secondary consideration, which we will discuss later. (There is a larger fractional change due to screening in the rates of lighter elements since for a given transition, given inner-shell electrons experience a potential which is more and more Coulomb-type with increasing Z.)

We can therefore begin our discussion of the influence of screening with the simpler nonrelativistic dipole calculation. This is quite sufficient in understanding the origins of the dominant screening effects of the relativistic cases as well. Both the Coulomb transition energy and dipole matrix element for the $2p\rightarrow 1s$ case are significantly reduced by screening. Analytic and numerical results show that the change of the dipole matrix element M is smaller than what would follow from the change in normalization constants alone. This is because wave-function shape terms lead to an increase in M. Figure 3 shows the ratios of the nonrelativistic screened and Coulomb wave functions as functions of the distance from the nucleus. The value at the nucleus ($ar=0$) gives the ratio of screened to Coulomb normalization. Lighter elements are more affected by screening, but not the scaled position (in ar) at which screening changes from decreasing to increasing the wave function. We also note from Fig. 3 that the $2p$ wave function is affected much more by screening (in other words, the $1s$ wave function is more Coulomb-like); the screening effect on M is determined largely by the behavior of the $2p$ wave function. At small distances the screened wave function is smaller than the Coulomb wave function (normalization effect) while at large distances the screened wave function is larger (since reduced binding energy in the screened case leads to a slower exponential decay rate, despite the fact that except for $n=l+1$ extra powers of r in the asymptotic Coulomb wave function must be compensated).

For the nodeless $2p$ wave function, the crossover from decrease due to screening to increase due to screening occurs at $ar\sim 6$ while the maximum in this wave function is at $ar=4$. The change with screening in the value of the matrix element suggests that the dominant distances of the integrand

TABLE II. Fractional change of point Coulomb transition rates due to screening for sample elements. (a) Using a nonrelativistic self-consistent potential (Herman-Skillman with the Slater exchange term and Latter tail correction) and (b) using a relativistic self-consistent potential [Lieberman (Ref. 30) with the Kohn-Sham exchange term and Latter tail correction].

		Nonrelativistic	Relativistic		
	Z	$2p\rightarrow 1s$	$K\alpha_1$	$K\alpha_2$	KL_1
(a)	92	−11.5%	−11%	−8.0%	−15%
	82	−12.5	−13	−10	−17
	50	−19	−20	−18.5	−29
	26	−29	−32	−31	
(b)	92	−14%	−15%	−11%	−20%
	82	−15	−16	−13	−21
	50	−21	−22	−20	−32
	26	−30	−35	−33	

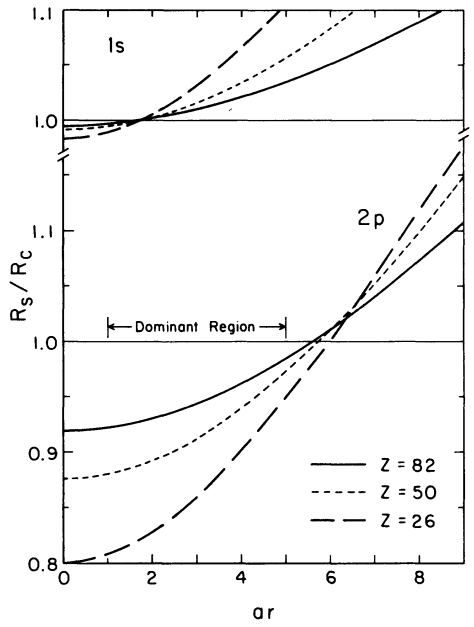

FIG. 3. Ratio of nonrelativistic screened radial bound-state wave function R_s to the corresponding Coulomb wave function R_c, for $1s$ and $2p$, versus radial distance scaled by $a=\alpha Z$. for nuclear charges $Z=26$, 50, and 82. The maximum in $R_c(2p)$ and the dominant region in the integrand of the $2p$-$1s$ matrix element are indicated.

are neither large nor small, generally before the $2p$ maximum and definitely before the crossover to screening enhancement of the wave function. In the Coulomb case we can make an easy estimate of this dominant region in the nonrelativistic length-form dipole matrix element. Integration from $ar=0$ to $ar=6$ indeed gives 95% of the total value, and we can therefore see how screening reduces the matrix element. (Note that screening need not cause a decrease in all such matrix elements M. For example, the screened matrix element for the same-shell transition, $2p\rightarrow 2s$ is larger than the Coulomb matrix element.[27] Here the dominant region is farther out from the nucleus than for $2p\rightarrow 1s$ and the crossover of $2s$, with a substantial screening effect, occurs still earlier than for $2p$. Consequently, while considering the cancellation effects of the $2s$ node, in the important region of integration the screened wave functions are greater than their Coulomb counterparts. Of course the Coulomb rate for $2p\rightarrow 2s$ vanishes, since screening is needed to remove the Coulomb degeneracy of the levels and produce a finite transition energy.)

There is a larger fractional decrease due to screening in the KL_1 transition rates compared to those of the other two transitions. This appears to reflect the importance of a dominant region closer to the nucleus for the $2s_{1/2}\rightarrow 1s_{1/2}$ matrix element. In such a region the normalization effect predominates, and indeed we get improved results by using more accurate normalization constants. However, due to the node in the $2s$ wave function, so that, in fact, the nonrelativistic Coulomb radial dipole matrix element vanishes, as well as due to the general vanishing of the nonrelativistic dipole matrix element from angular momentum considerations, it is more difficult to give a simple and gauge invariant discussion of the important regions in the determination of the matrix element.

The screening effects on both the transition energy and the length form of the dipole matrix element must be considered simultaneously. The spacing between these inner-shell levels is decreased by screening [as predicted in APT, where the $2p\rightarrow 1s$ transition energy is $(3a^2/8)(1-\frac{28}{3}\Lambda_2-72\Lambda_3)$] and hence transition energies become smaller (except, as already noted, those involving levels belong to the same shell). This can be understood from the same type of argument as for the matrix element, as the $2p$ energy, given as the expectation value of the Hamiltonian, will be determined where the wave function is large, i.e., where screening causes reductions in both the wave function and the Hamiltonian. The nonrelativistic results of Eq. (24) indicate, with the choice of gauge leading to the length form of the matrix element, that comparable screening effects come from the matrix element and from the transition energy.

If now we try to understand the differences between screening effects on the nonrelativistic rates and screening effects on the relativistic rates, one part of the difference arises from the fact that we are dealing with different screened potentials in the two calculations. This corresponds to the well-known relativistic contraction of the charge distribution of inner-shell electrons. This type of difference in screening effects on relativistic and nonrelativistic rates can be identified by performing the complete relativistic calculation of the single-electron transition for relativistic wave functions in the nonrelativistic rather than the relativistic screened potential, and vice versa. Comparative data from such calculations are included in Tables I and II. These results indicate that the difference in potential causes a small change (roughly proportional to Z) amounting to approximately a 3% in-

crease in the rates of high-Z elements when a nonrelativistic rather than a relativistic self-consistent central potential is used. Within the analytic perturbation theory, this change in potential is manifested as a change in the scale parameter λ, with little change in the potential shape or, equivalently, in the V coefficients. Since $\lambda_{\text{rel}} > \lambda_{\text{nonrel}}$, the change is a contraction in scale. Increasing λ (as in the switch to the relativistic potential) provides more screening, which for these K-L transitions reduces rates.

Even in the same potential, Table II shows that there is some difference in the screening effects on relativistic and nonrelativistic transitions. One feature is that for high-Z elements there is a lessened importance of screening on the $K\alpha_2$ rates, as compared to the $K\alpha_1$ which exhibit screening effects similar to those of the nonrelativistic $2p \rightarrow 1s$ rate. In order to understand this we show in Fig. 4 the screening effects on the large and small components of the $2p_{3/2,1/2}$ wave functions, as well as on the nonrelativistic $2p$ wave function in the same relativistic self-consistent central potential. (We should not expect to easily understand differences in relativistic and nonrelativistic rates from comparisons of the curves, as they enter into different matrix elements.) The contraction and greater screening of the atom (increase in λ) would tend to decrease relativistic normalizations more than screening decreases the nonrelativistic values. The increase in λ also means that screening reduces the

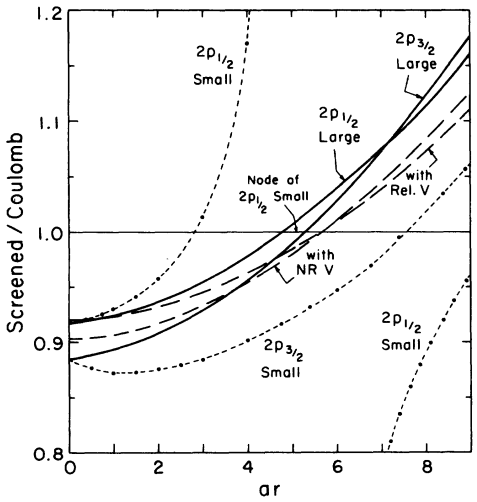

FIG. 4. Same as Fig. 3 but with large and small component bound-state wave functions, for the $2p_{3/2}$ and $2p_{1/2}$ ($Z=82$) cases. The corresponding nonrelativistic $2p$ case is also shown, both as obtained with the nonrelativistic and with relativistic potentials.

larger relativistic Coulomb binding energies more than the smaller nonrelativistic Coulomb binding energies. However, in comparison to $2p_{3/2}$, the $2p_{1/2}$ wave function is pulled in (particularly for large Z) by its r^{γ} behavior at small distances, so that its dominant region occurs at a smaller distance where the potential is more Coulomb-like and hence its normalization differs less from the Coulomb case. The $2p_{1/2}$ wave function also makes the transition to enhancement by screening much sooner, and so for a similar dominant region screening has less effect on the rate than in the $2p_{3/2}$ case. The very different effect of screening at small distances on the small components in the two cases is related to the presence (and shift with screening) of a node in the $2p_{1/2}$ small component. Asymptotically, the ratio of small to large components is $[(1-E)/(1+E)]$, where E is the Coulomb or screened binding energy. Since the screened binding energy is less than the Coulomb binding energy, it follows that asymptotically the ratio of screened-Coulomb small components is smaller than the ratio of screened-Coulomb large components.

Next we proceed to consider, for a given choice of potential (Coulomb or screened), the difference between the usual nonrelativistic dipole calculation without retardation and the full relativistic multipole calculation with retardation. The easiest aspect of this comparison to discuss is the role of the higher multipoles, since for bound-bound transitions only a few multipoles of the radiation field are allowed by the conservation rules for transitions between states of definite n, j, and l. In fact, for KL transitions, only $K\alpha_1$ has a higher multipole ($M2$) contribution to the transition rate, negligible for low Z and only reaching 1% (additive) by $Z=92$. The magnitudes of higher multipole contributions can be estimated readily by realizing that there is no interference between multipole matrix elements in a transition rate (as contrasted to an angular distribution or polarization correlation). When K is small, the next multipole gives a matrix element of relative order K, and so a contribution to the rate of relative order $K^2=O(a^4)$. Even for uranium ($Z=92$) this contribution is small since with $a=0.67$, $K \sim 3a^2/8$ for the KL transition, and $K^2 \sim 0.03$. Hence, even for inner-shell transitions of heavy elements, higher multipoles give minor contributions except in the case of forbidden transitions. [For photoeffect the same argument suggests that higher multipole contributions to the total cross section generally be-

TABLE III. Ratio R of relativistic to nonrelativistic transition rates and scaled deviation δ, $R \equiv 1+\delta a^2$ and shown as $R(\delta)$, for sample elements. The same relativistic potential was used in the screened relativistic and nonrelativistic rates.

	Transition $K\alpha_1$		Transition $K\alpha_2$	
Z	Screened	Coulomb	Screened	Coulomb
92	0.881(−0.264)	0.880(−0.266)	1.102(0.228)	1.052(0.116)
82	0.908(−0.258)	0.908(−0.257)	1.081(0.220)	1.043(0.120)
50	0.957(−0.323)	0.968(−0.237)	1.021(0.160)	1.016(0.119)
26	0.958(−1.16)	0.992(−0.236)	0.980(−0.69)	1.006(0.167)

come large only for photon energies above 150 keV ($K \sim 0.3$) while for the angular distribution, such effects become large for K above 25 keV ($K \sim 0.05$), i.e., even down to threshold for the K and L shells of high-Z elements.]

Although we have written an expression for the radial matrix element in a fashion which seemingly would permit an investigation of retardation independently of relativistic effects, it must be realized that, in fact, gauge invariance provides a connection between these two features. As a result different forms of the matrix element (see, for example, Refs. 11, 13, and 16) are physically equivalent, though they would not be if one took nonretarded (small-K) or nonrelativistic (small-a^2) limits independently. If we simultaneously expand for small retardation and for nonrelativistic wave functions (see Grant[11]) we are led to nonrelativistic dipole matrix elements. Grant has shown, in general, that the first corrections are of order α^2 and not of order α. We have given in Eqs. (24a) and (24b) these corrections in $O(a^2)$ for the $K\alpha$ transitions in the Coulomb case, while in Eq. (24c) we have summed the rates to see the correction to the nonrelativistic value. We have shown the numerical ratios (Coulomb and screened) of relativistic and nonrelativistic rates in Table III and have obtained the deviations scaled with a^2. While the effects are indeed of $O(a^2)$, unlike those from higher multipole contributions, the coefficients are relatively small, so that even for the high-Z inner-shell transitions the nonrelativistic dipole approximation remains fairly good. This same feature, that for a multipole matrix element relativistic and retardation effects (combined) remain small, has been observed in s-state photoeffect[28] and other processes.

ACKNOWLEDGMENTS

This work was supported in part by the National Science Foundation. One of the authors (S.C.) wishes to acknowledge support through an A. W. Mellon predoctoral fellowship.

APPENDIX

A. Analytic wave functions, energies, and normalizations for the K and L shells

The radial wave functions, f (upper or large component) and g (lower or small component) are written in terms of the reduced radial functions F_1 and F_2 in Eq. (7). In the following discussion we will write the reduced radial functions, energy eigenvalues and normalization constants in the forms

$$F_1(r)=F_{1c}(r)+A_2(r)\Lambda_2+A_3(r)\Lambda_3 ,$$

$$F_2(r)=F_{2c}(r)+B_2(r)\Lambda_2+B_3(r)\Lambda_3 ,$$

$$E=E_c-a^2(\Lambda_1+e_2\Lambda_2+e_3\Lambda_3) ,$$

$$N=N_c(1-n_2\Lambda_2-n_3\Lambda_3) ,$$

where $\Lambda_n=V_n\lambda^n a^{-n}$. We also let $t=\gamma+1$ and $s=2\gamma+1$ where $\gamma=(\kappa^2-a^2)^{1/2}$.

1. K shell ($1s_{1/2}$), $\kappa=-1$, $x=2ar$. We have the following:

$$F_{1c}=0,\quad A_2=\mu x/4,\quad A_3=A_2(t+x/2) ,$$

$$F_{2c}=\mu,\quad B_2=-A_2(b-\gamma x/2),$$

$$B_3=-A_2(bt-x/2-\gamma x^2/6) ,$$

where $\mu=2\gamma^{1/2}$ and $b=2\gamma^2+\gamma-2$. Also,

$$E_c=\gamma,\quad e_2=s/2,\quad e_3=st/2 ,$$

$$N_c=\frac{(2a)^{s/2}}{\mu[\Gamma(s)]^{1/2}},\quad n_2=(2-\gamma)e_3/2 ,$$

$$n_3=(9+6\gamma-4\gamma^2)e_3/6 .$$

2. L_1, L_2 subshells ($2s_{1/2}$,$2p_{1/2}$), $\kappa=\pm 1$, $x=2ar/\eta'$, $\eta'=(2t)^{1/2}$. [Upper (lower) signs refer

to the L_2 (L_1) subshell.]

We have

$$F_{1c}=-w,\quad A_2=-tx(a_0+a_1x)/4w,$$

$$A_3=-t^2x(b_0+b_1x+b_2x^2)/2w\ ,$$

where

$$w=(\eta'\pm1)^{1/2}\ ,$$

$$a_0=\pm(11+3\gamma-6\gamma^2)+(7-5\gamma-6\gamma^2)\eta'\ ,$$

$$a_1=(\gamma+3)\eta'\pm t\ ,$$

$$b_0=(9+2\gamma-4\gamma^2)\eta'+(11-10\gamma-8\gamma^2)t\ ,$$

$$b_1=4\gamma+7\pm2\eta',\quad b_2=(\gamma+4\pm\eta'/2)/3\ .$$

Also,

$$F_{2c}=(t-x)/w,$$

$$B_2=-tx(c_0+c_1x+c_2x^2)/4w\ ,$$

$$B_3=-t^2x(d_0+d_1x+d_2x^2+d_3x^3)/2w\ ,$$

where

$$c_0=12\gamma^3+16\gamma^2-7\gamma-13\pm2t\eta'\ ,$$

$$c_1=2(1-4\gamma)t\pm\eta',\quad c_2=t\ ,$$

$$d_0=(8\gamma^3+14\gamma^2-3\gamma-12)\eta'\pm(6\gamma+1)t\ ,$$

$$d_1=\pm3\gamma-(4\gamma+5)\eta'\gamma\ ,$$

$$d_2=(5-2\gamma)\eta'/6,\quad d_3=\eta'/6\ .$$

Also,

$$E_c=\eta'/2,\quad e_2=[(6\gamma+5)\eta'\pm2]/4\ ,$$

$$e_3=(4\gamma^2\pm9\gamma+5\pm3\eta'/2)t\ ,$$

and

$$N_c=\frac{(2a/\eta')^{s/2}}{[2\eta'\Gamma(s)]}\ ,$$

$$n_2=(-8\gamma^3+8\gamma^2+37\gamma+17\pm3\eta'\gamma)t/4\ ,$$

$$n_3=[-20\gamma^3+30\gamma^2+149\gamma+84\pm3(8\gamma-9)\eta'/2]t^2\eta'/6\ .$$

3. L_3 subshell ($2p_{3/2}$), $\kappa=-2$, $x=ar$, $\gamma=(4-a^2)^{1/2}$. We have the following:

$$F_{1c}=0,\quad A_2=2\tau x\ ,$$

$$A_3=2\tau x(2t+x),\quad \tau=2(2\gamma)^{1/2}\ ,$$

$$F_{2c}=\tau,\quad B_2=-A_2(\beta-\gamma x/4)\ ,$$

$$B_3=-A_2(2\beta t-2x-\gamma x^2/6)\ ,$$

$$\beta=\gamma^2+\gamma/2-4\ .$$

Also,

$$E_c=\gamma/2,\quad e_2=s,\quad e_3=2st\ ,$$

and

$$N_c=\frac{a^{s/2}}{2[2\gamma\Gamma(s)]^{1/2}},\quad n_2=(8+\gamma-\gamma^2)s\ ,$$

$$n_3=4(18+3\gamma-2\gamma^2)st/3\ .$$

4. Nonrelativistic limits. In the nonrelativistic limit ($a^2<<1$), these radial wave functions and energy eigenvalues reduce to the corresponding solutions derived by McEnnan *et al.*[29] in the nonrelativistic version of the APT. One can verify that $f\rightarrow rR$ and $g\rightarrow(d/dr+\kappa/r)rR/2$, where R is the radial solution to the Schrödinger equation.

B. The integrals $I_{ij}^{(L)}$

Consider

$$I_{ij}^{(L)}\equiv\int_0^\infty j_L(Kr)e^{-(p_{ca}+p_{cb})r}r^{\gamma_a+\gamma_b}F_i^{(b)}F_j^{(a)}dr\ .$$

We let

$$C_n^{(L)}=a^n\int_0^\infty j_L(Kr)e^{-(p_{ca}+p_{cb})r}r^{\gamma_a+\gamma_b+n}dr\ ,$$

which can be evaluated directly for any n and $L=0,1,2$ (the only ones that are needed in this calculation) by using the formulas given in Eq. (12a)–(12c). One gets the explicit results shown below (keeping up to order λ^3 and following the notation in the Appendix, Sec. A).

1. Transition $K\alpha_1(2p_{3/2}\rightarrow1s_{1/2})$. We have the following:

$$I_{11}^{(L)}=(\lambda^4),\quad I_{12}^{(L)}=2\sigma[C_1^{(L)}\Lambda_2+(C_1^{(L)}t_b+C_2^{(L)})\Lambda_3],\quad \sigma=(2\gamma_a\gamma_b)^{1/2},\quad I_{21}^{(L)}=8\sigma[C_1^{(L)}\Lambda_2+(2C_1^{(L)}t_a+C_2^{(L)})\Lambda_3]\ ,$$

$$I_{22}^{(L)}=4\sigma\{C_0^{(L)}-\tfrac{1}{2}[2\gamma_as_a+\gamma_bs_b-18)C_1^{(L)}-(\gamma_a+\gamma_b)C_2^{(L)}]\Lambda_2-\tfrac{1}{4}[4(\gamma_as_a-8)t_aC_1^{(L)}+(\gamma_bs_b-2)t_bC_1^{(L)}-9C_2^{(L)}-2(\gamma_a+\gamma_b)C_3^{(L)}/3]\Lambda_3\}\ .$$

2. *Transitions* $K\alpha_2$, KL_1 ($2p_{1/2},2s_{1/2}\rightarrow 1s_{1/2}$). [Upper (lower) signs refer to the $K\alpha_2(KL_1)$ transition]:

$$I_{11}^{(L)}=-u[C_1^{(L)}\Lambda_2+(tC_1^{(L)}+C_2^{(L)})\Lambda_3],$$

$$I_{12}^{(L)}=\frac{u}{v}\{(s\eta' C_1^{(L)}-2C_2^{(L)})\Lambda_2+[st\eta' C_1^{(L)}-(2t-\eta' s)C_2^{(L)}-2C_3^{(L)}]\Lambda_3\},$$

$$I_{21}^{(L)}=-2u\left[C_0^{(L)}+\frac{\eta'}{2v}(q_1C_1^{(L)}+q_2C_2^{(L)})\Lambda_2+\frac{\eta'}{2v}(r_1C_1^{(L)}+r_2C_2^{(L)}+r_3C_3^{(L)})\Lambda_3\right],$$

where

$$q_1=-(6\gamma^2+5\gamma-7)t-(2\gamma^2+\gamma-2)(\eta'\pm 1)\mp(6\gamma^2-3\gamma-11)\eta'/2,\quad q_2=(2\gamma+3)\eta'\pm s,$$

$$r_1=-[(8\gamma^3+20\gamma^2-13)\eta'\pm(8\gamma^3+6\gamma^2-21\gamma-20)]s,\quad r_2=2(4\gamma^2+11\gamma+7)\pm 1+(1\pm 4t)\eta',$$

$$r_3=2[2(\gamma+2)\eta'\pm s]/3.$$

Also,

$$I_{22}^{(L)}=-\frac{u}{v}[2(2C_1^{(L)}-\eta' sC_0^{(L)})+(Q_1C_1^{(L)}+Q_2C_2^{(L)}+Q_3C_3^{(L)})\Lambda_2+(R_1C_1^{(L)}+R_2C_2^{(L)}+R_3C_3^{(L)}+R_4C_4^{(L)})\Lambda_3],$$

where

$$Q_1=(12\gamma^3+16\gamma^2-7\gamma-13)t-[(2\gamma^2+\gamma-2)s\pm 2t^2]\eta',$$

$$Q_2=-(10\gamma^2+7\gamma-2)\eta'-2(2\gamma^2+\gamma-2)\pm 2t,\quad Q_3=2s,$$

$$R_1=(16\gamma^4+48\gamma^3+26\gamma^2-33\gamma-26)t\quad\mp 2(6\gamma+1)t^3,$$

$$R_2=-2t(8\gamma^3+20\gamma^2+11\gamma-2\mp 3\gamma\eta'),\quad R_3=\tfrac{2}{3}[3-(4\gamma^2-2\gamma-5)\eta'],\quad R_4=4s/3.$$

[1]H. S. W. Massey and E. H. S. Burhop, Proc. Cambridge Philos. Soc. 32, 461 (1936).
[2]H. S. W. Massey and E. H. S. Burhop, Proc. Soc. London Ser. A 153, 661 (1936).
[3]W. Laskar, J. Phys. Radium 16, 644 (1955).
[4]W. Laskar, Ann. Phys. (Paris) 13, 258 (1958).
[5]W. B. Payne and J. S. Levinger, Phys. Rev. 101, 1020 (1956).
[6]W. N. Assad, Proc. Soc. London Ser. A 249, 555 (1959).
[7]G. R. Taylor and W. B. Payne, Phys. Rev. 118, 1549 (1960).
[8]F. A. Babushkin, Acta. Phys. Pol 25, 749 (1964).
[9]F. A. Babushkin, Opt. Spectrosk. 19, 3 (1965) [Opt. Spectrosc. (USSR) 19, 1 (1965)].
[10]F. A. Babushkin, Acta. Phys. Pol. 31, 459 (1967).
[11]I. P. Grant, J. Phys. B 7, 1458 (1974).
[12]R. H. Garstang, in *Topics in Modern Physics,* edited by W. E. Brittin and H. Odabasi (Colorado Associated University Press, Boulder, 1971).
[13]H. R. Rosner and C. P. Bhalla, Z. Phys. 231, 347 (1970).
[14]R. Anholt and J. O. Rasmussen, Phys. Rev. A 9, 585 (1974).
[15]C. C. Lu, F. B. Malik, and J. A. Carlson, Nucl. Phys. A175, 289 (1971).
[16]J. H. Scofield, Phys. Rev. 179, 9 (1969).
[17]J. H. Scofield, in *Atomic Inner-Shell Processes,* edited by B. Crasemann (Academic, New York, 1975), Vol. I.
[18]J. H. Scofield, Phys. Rev. A 9, 1041 (1974).
[19]J. McEnnan, D. J. Botto, R. H. Pratt, D. Bunaciu,

and V. Florescu, Phys. Rev. A 16, 1768 (1977).
[20]H. J. Rose and D. M. Brink, Rev. Mod. Phys. 39, 306 (1967).
[21]G. Breit and E. Teller, Astrophys. J. 91, 215 (1940).
[22]I. P. Grant, Adv. Phys. 19, 747 (1970).
[23]W. R. Johnson, Phys. Rev. Lett. 29, 1123 (1972).
[24]R. Marrus and R. W. Schnieder, Phys. Rev. A 5, 1160 (1972).
[25]M. H. Prior, Phys. Rev. Lett. 29, 611 (1972).
[26]C. A. Kocher, J. E. Clendenin, and R. Novick, Phys. Rev. Lett. 29, 615 (1972).
[27]Y. S. Kim, S. D. Oh, and R. H. Pratt, Phys. Rev. A 18, 194 (1978).
[28]S. D. Oh, J. McEnnan, and R. H. Pratt, Phys. Rev. A 14, 1428 (1976).
[29]J. McEnnan, L. Kissel, and R. H. Pratt, Phys. Rev. A 13, 532 (1976).
[30]D. Liberman, J. T. Waber, and D. T. Cromer, Phys. Rev. A 27, 137 (1965).